Received: 20 September 2018 | Revised: 29 November 2018 | Accepted: 5 December 2018
DOI: 10.1002/ardp.201800278

FULL PAPER

DPhG ARCH PHARM
Archiv der Pharmazie

Bi-heterocyclic benzamides as alkaline phosphatase inhibitors: Mechanistic comprehensions through kinetics and computational approaches

Muhammad A. Abbasi[1,2] | Majid Nazir[2] | Aziz ur-Rehman[2] | Sabahat Z. Siddiqui[2] | Mubashir Hassan[1] | Hussain Raza[1] | Syed A. A. Shah[3] | Muhammad Shahid[4] | Sung-Yum Seo[1]

[1] Department of Biological Sciences, College of Natural Sciences, Kongju National University, Gongju, South Korea

[2] Department of Chemistry, Government College University, Lahore, Pakistan

[3] Faculty of Pharmacy and Atta-ur-Rahman Institute for Natural Products Discovery (AuRIns), Level 9, FF3, Universiti Teknologi MARA, Puncak Alam Campus, Selangor Darul Ehsan, Malaysia

[4] Department of Biochemistry, University of Agriculture, Faisalabad, Pakistan

Correspondence
Dr. Muhammad A. Abbasi, Department of Chemistry, Government College University, Lahore-54000, Pakistan.
Email: abbasi@gcu.edu.pk

Prof. Dr. Sung-Yum Seo, Department of Biological Sciences, College of Natural Sciences, Kongju National University, Gongju 32588, South Korea.
Email: dnalove@kongju.ac.kr

Funding information
National Research Foundation of Korea, Grant number: 2017R1D1A1B03034948

Abstract

Novel bi-heterocyclic benzamides were synthesized by sequentially converting 4-(1*H*-indol-3-yl)butanoic acid (**1**) into ethyl 4-(1*H*-indol-3-yl)butanoate (**2**), 4-(1*H*-indol-3-yl)butanohydrazide (**3**), and a nucleophilic 5-[3-(1*H*-indol-3-yl)propyl]-1,3,4-oxadiazole-2-thiol (**4**). In a parallel series of reactions, various electrophiles were synthesized by reacting substituted anilines (**5a–k**) with 4-(chloromethyl)benzoylchloride (**6**) to afford 4-(chloromethyl)-*N*-(substituted-phenyl)benzamides (**7a–k**). Finally, the nucleophilic substitution reaction of **4** was carried out with newly synthesized electrophiles, **7a–k**, to acquire the targeted bi-heterocyclic benzamides, **8a–k**. The structural confirmation of all the synthesized compounds was done by IR, ^{1}H NMR, ^{13}C NMR, EI-MS, and CHN analysis data. The inhibitory effects of these bi-heterocyclic benzamides (**8a–k**) were evaluated against alkaline phosphatase, and all these molecules were identified as potent inhibitors relative to the standard used. The kinetics mechanism was ascribed by evaluating the Lineweaver–Burk plots, which revealed that compound **8b** inhibited alkaline phosphatase non-competitively to form an enzyme–inhibitor complex. The inhibition constant K_i calculated from Dixon plots for this compound was 1.15 μM. The computational study was in full agreement with the experimental records and these ligands exhibited good binding energy values. These molecules also exhibited mild cytotoxicity toward red blood cell membranes when analyzed through hemolysis. So, these molecules might be deliberated as nontoxic medicinal scaffolds to render normal calcification of bones and teeth.

KEYWORDS
benzamides, bi-heterocyclic, kinetics, molecular docking, phosphatase

1 | INTRODUCTION

Indole is composed of a benzo-pyrrole in which the benzene and pyrrole rings are fused together through the 2- and 3-positions of the pyrrole ring.[1] Indoles are found in various natural products and have been identified as products of chemical and biological importance. Indole is a highly conserved heterocyclic molecule that acts as a free radical scavenger and has a broad spectrum of antioxidant activity.

Indole core is also an important component in many of recent drugs for treatment of chemotherapy-induced nausea and vomiting, cluster headache, or as antihypertensive, antineoplastic, and antimitotic agents.[2–4]

1,3,4-Oxadiazoles derivatives have played a significant role in medicinal chemistry. Considerable attention has been focused on 2,5-disubstituted-1,3,4-oxadiazole containing compounds due to their remarkable biological activities. Such compounds have been recognized as antibacterial, anticancer, anti-Parkinson, anti-HIV, and anti-proliferative agents.[5–8]

Benzamides have been reported as muscle relaxants and activators of potassium channel. These are also exploited as analgesic, anti-inflammatory, and antihelmintic agents.[9,10] Some heterocyclic benzamides have shown activity in central nervous system while others act as anti-psychotics, anti-emetics, and gastric motility stimulants.[11–13]

Alkaline phosphatase (ALP; E.C.3.I.3.1.) is a ubiquitous membrane-bound glycoprotein that catalyzes the hydrolysis of phosphate monoesters at basic pH values. Alkaline phosphatase is divided into four isozymes depending upon the site of tissue expression that are intestinal ALP, placental ALP, germ cell ALP, and tissue-nonspecific alkaline phosphatase or liver/bone/kidney (L/B/K) ALP. Mammalian alkaline phosphatases (ALPs) are zinc containing metalloenzymes encoded by a multigene family and function as dimeric molecules. Three metal ions including two Zn^{+2} and one Mg^{+2} in the active site are essential for enzymatic activity. However, these metal ions also contribute substantially to the conformation of the ALP monomer and indirectly regulate subunit–subunit interactions. Although ALPs are present in many mammalian tissues and have been studied for the last several years, still little is known about them.[14] High concentrations of tissue-nonspecific alkaline phosphatase (TNAP) have been found in mineralizing tissues such as bones and teeth, where role of TNAP is essential for normal bone formation. Overexpression of TNAP has been known to cause abnormal calcification including vascular calcification and leads to increased deposition of mineral hydroxyapatite causing hydroxyapatite deposition disorder (HADD). A decrease in concentration of extracellular ATP via TNAP inhibition has been recognized to be essential for neuronal development and synaptic function. A number of Alzheimer's disease patients have indicated considerable elevated TNAP activity in the hippocampus section of brain. TNAP can therefore be explored as a potential target for treatment of neurological disorders.[15–18]

Our group has already reported lead compounds based on indole and oxadiazole scaffold as enzyme inhibitors,[19,20] and the current study was expanded to explore new therapeutic potentials of such hybrid molecules as alkaline phosphatase inhibitors. *In silico* studies were also carried out to ascertain different types of interactions with active pocket of enzyme. Moreover, their cytotoxicity was also assessed to find their utility as harmless drug candidates in drug discovery and development.

2 | RESULTS AND DISCUSSION

2.1 | Chemistry

The convergent synthesis of targeted *N*-substituted derivatives was accomplished in very good yields through several steps. First, the 4-(1*H*-indol-3-yl)butanoic acid (**1**) was subjected to esterification by ethanol in the presence of concentrated sulfuric acid taken in catalytic amount. Ethanol was used as reactant and also as a solvent in order to push the equilibrium toward product side, as it was a reversible reaction. The product was collected by solvent extraction after the addition of a weak base and excess of water. The base was added to neutralize the catalytic sulfuric acid and the unreacted carboxylic acid. The salts of these acids were partitioned to the aqueous layer while the resulted ester to the organic phase during solvent extraction. Thus, ethyl 4-(1*H*-indol-3-yl)butanoate (**2**) was obtained as brownish liquid (solid at refrigeration).[19,20] The second step was performed to convert this ethyl ester to respective carbohydrazide, **3**, by the nucleophillic hydrazine in the presence of an organic solvent like methanol and refluxed for 14 h. Thus, 4-(1*H*-indol-3-yl)butanohydrazide (**3**) was obtained as a light brown-colored solid.[14,15] The third step was a cyclization to form heterocyclic ring through reaction with CS_2 in a basic alcoholic medium. The resulting product was 5-[3-(1*H*-indol-3-yl)-propyl]-1,3,4-oxadiazole-2-thiol (**4**) having a mercapto group at its second carbon.[14,15] In a parallel phase of reactions, different electrophiles were synthesized by reacting substituted anilines (**5a–k**) with 4-(chloromethyl)benzoyl chloride (**6**) to afford 4-(chloromethyl)-*N*-(substituted-phenyl)benzamides (**7a–k**).[21] Then in the last step, acidic proton of **4** was replaced with different electrophiles, **7a–k**, in the presence of LiH base using aprotic polar medium to get required bi-heterocyclic benzamide derivatives, **8a–k**, as sketched in Scheme 1 and different groups are listed in Table 1.

The structural analysis of one of the compounds is discussed hereby in detail for the benefit of the reader. The molecule **8f** was obtained as yellow-colored amorphous powder. Its molecular formula, $C_{28}H_{26}N_4SO_2$, was established through the molecular ion peak at *m/z* 482 in its EI-MS spectrum and by CHN analysis data. The count of the number of protons in its ^{1}H NMR spectrum and number of carbon resonances in its ^{13}C NMR spectrum was also in agreement with its deduced molecular formula. Different functionalities in this molecule were depicted by absorption bands in its IR spectrum at ν 3317 (N-H str.), 2955 (C-H aromatic str.), 1654 (CO str.), 1599 (C═C aromatic str.), 1535, 1484, 1449 (str. for oxadiazole), 1155 (C-O-C str.), 1103 (CN str.), 681 (C-S str.) cm^{-1}. With the help of ^{1}H NMR spectrum of this molecule, the indole heterocyclic core was identified clearly by the characteristic signals at δ 10.82 (s, 1H, NH-1), 7.51 (br.d, *J* = 7.6 Hz, 1H, H-7), 7.35 (br.d, *J* = 8.0 Hz, 1H, H-4), 7.16–7.14 (m, 3H, H-2, H-2‴ & H-6‴), 7.06 (br.t, *J* = 7.2 Hz, 1H, H-6) and 6.97 (br.t, *J* = 7.2 Hz, 1H, H-5) ppm. Similarly, the resonance at δ 7.65 (br.d, *J* = 7.9 Hz, 2H, H-3‴ & H-5‴), a merged signal at δ 7.16–7.14 (m, 3H, H-2, H-2‴ & H-6‴), along with one methyl signal at δ 2.09 (s, 3H, CH_3-4‴) ppm, were altogether typical for a 4-methylphenyl group in the molecule. The *C*

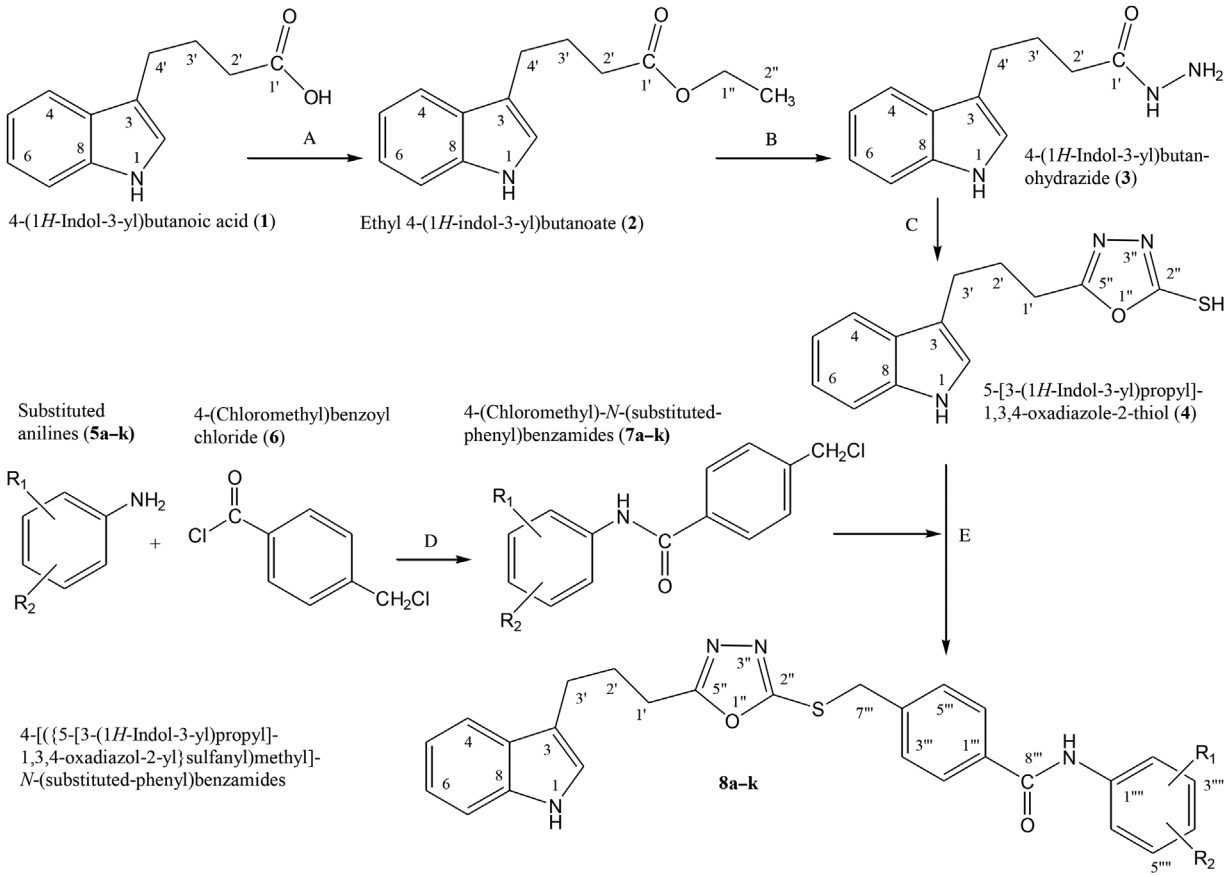

SCHEME 1 Outline for the synthesis of 4-[({5-[3-(1*H*-indol-3-yl)propyl]-1,3,4-oxadiazol-2-yl}sulfanyl)methyl]-*N*-(substituted-phenyl)-benzamides (**8a–k**). Reagents and conditions: (A) EtOH/H_2SO_4/refluxing for 8 h. (B) MeOH/$N_2H_4 \cdot H_2O$/refluxing for 14 h. (C) EtOH/CS_2/KOH/refluxing for 16 h. (D) Aq. Na_2CO_3 soln./pH 9–10/stirring at RT for 20–30 min. (E) DMF/LiH/stirring for 40–50 h

and *N*-substituted 4-yl-methylbenzamido group was identified by four signals at δ 10.16 (s, 1H, CONH), 7.91 (br.d, *J* = 7.9 Hz, 2H, H-2‴ & H-6‴), 7.57 (br.d, *J* = 7.8 Hz, 2H, H-3‴ & H-5‴) and 4.54 (s, 2H, CH_2-7‴). In the up-field region of spectrum, the signals of three intervening methylene groups at δ 2.86 (t, *J* = 7.2 Hz, 2H, CH_2-1′), 2.77 (t, *J* = 7.1 Hz, 2H, CH_2-3′), and 2.05 (quint., *J* = 7.2 Hz, 2H, CH_2-2′), were helpful to ascertain the connectivity of indole moiety from its 3-position to the 5-position of oxadiazole scaffold. The ^{1}H NMR spectrum of this compound and its expanded zones are shown in Figure 1(a–c).

TABLE 1 Different groups (-R_1 and -R_2) in Scheme 1

Compd.	-R_1	-R_2	Compd.	-R_1	-R_2
5a, **7a**, **8a**	3-OC_2H_5	-H	**5g**, **7g**, **8g**	2-CH_3	3-CH_3
5b, **7b**, **8b**	4-OC_2H_5	-H	**5h**, **7h**, **8h**	2-CH_3	4-CH_3
5c, **7c**, **8c**	2-C_2H_5	-H	**5i**, **7i**, **8i**	2-CH_3	6-CH_3
5d, **7d**, **8d**	2-CH_3	-H	**5j**, **7j**, **8j**	3-CH_3	4-CH_3
5e, **7e**, **8e**	3-CH_3	-H	**5k**, **7k**, **8k**	3-CH_3	5-CH_3
5f, **7f**, **8f**	4-CH_3	-H			

The carbon skeleton of this molecule was also fully supported by its ^{13}C NMR spectrum, shown in Figure 2. The ^{13}C NMR spectrum due to some symmetrical duplets depicted overall 24 carbon resonances, where the most downfield quaternary carbons signals at δ 168.09 (C-5″) and 162.29 (C-2″) belonged to the 1,3,4-oxadiazole ring, thus confirming its cyclization. The other three quaternary carbons appearing at δ 136.29 (C-8), 127.00 (C-9), and 113.22 (C-3) ppm were attributes of the indole core. The methine carbon resonances appearing at δ 122.49 (C-2), 120.86 (C-6), 118.18 (C-7), 118.16 (C-5), 111.35 (C-4) were also coherent with the indole moiety.[19] The dually substituted 4-yl-methylbenzamido group was confirmed by its discrete resonances, one for a carbonyl group at δ 164.90 (C-8‴), other four signals at δ 140.19 (C-4‴), 134.35 (C-1‴), 128.93 (C-3‴ & C-5‴), 127.80 (C-2‴ & C-6‴), and one signal of methylene group at δ 35.34 (C-7‴).[20] The 4-methylphenyl group attached with a nitrogen atom was thoroughly corroborated by two quaternary signals at δ 136.56 (C-1⁗) and 132.57 (C-4⁗), two methine signals at δ 128.88 (C-2⁗ & C-6⁗) and 120.31 (C-3⁗ & C-5⁗), along with one methyl signal at δ 20.46 (CH_3-4⁗). In the up-field region of the spectrum, three signals at δ 26.48 (C-2′), 24.26 (C-1′), and 23.81 (C-3′) were characteristic for three connected methylenes, which were joining the indole moiety with heterocyclic oxadiazole core in the molecule.[19] The salient connectivities in the carbon skeleton of this molecule were thoroughly

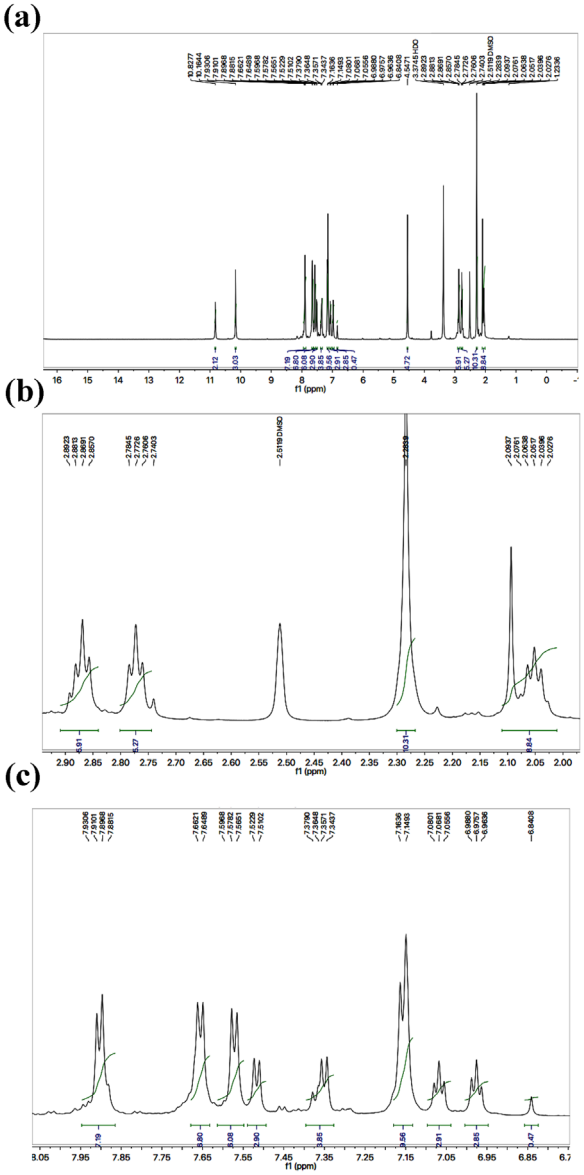

FIGURE 1 (a) ^{1}H NMR spectrum of **8f**. (b) Expanded aromatic region of ^{1}H NMR spectrum of **8f**. (c) Expanded aliphatic region of ^{1}H NMR spectrum of **8f**

substantiated by its HMBC spectrum. This spectrum, along with significant correlations, is shown in Figure 3. So, on the basis of aforesaid collective evidences, the structure of **8f** was confirmed and it was named as 4-[({5-[3-(1*H*-indol-3-yl)propyl]-1,3,4-oxadiazol-2-yl}-sulfanyl)methyl]-*N*-(4-methylphenyl)benzamide. A similar protocol was exercised for the structural characterization of other derivatives in the synthesized series.

2.2 | Alkaline phosphatase inhibition and structure–activity relationship (SAR)

The synthesized bi-heterocyclic benzamides (**8a–k**) were evaluated for their inhibitory potentials against alkaline phosphatase enzyme and

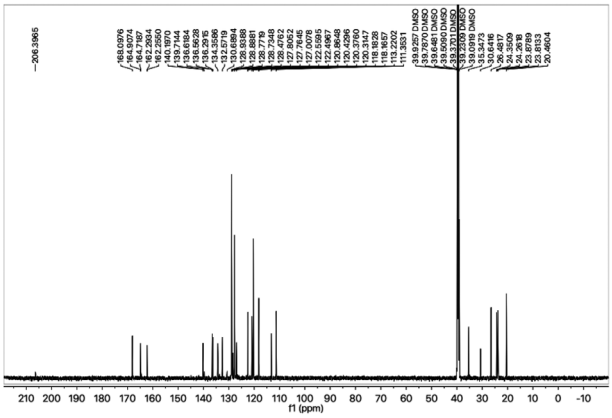

FIGURE 2 ^{13}C NMR spectrum of **8f** molecule

their results are presented in Table 2. All these compounds exhibited very potent inhibitory activities against this enzyme, as evident from their lower IC_{50} (μM) values, relative to standard, KH_2PO_4, having IC_{50} value of 5.2421 ± 0.4722 μM. Though the exposed activity is accumulative of a whole molecule, yet a limited SAR was predictable by discerning the effect of different aryl entity on the inhibitory potential, as it was the only varying part and all other parts were similar in all molecules. The general structural parts of the studied benzamides are accentuated in Figure 4.

The compounds **8a** and **8b** both contained an ethoxy group in the aryl part and exhibited very superb and comparable inhibitory activities, IC_{50} = 0.0676 ± 0.0057 and IC_{50} = 0.0427 ± 0.0167 μM, respectively. Moreover, **8b** bearing 4-ethoxy group was recognized as the most active compound in the synthetic series. It means, the presence of a medium-sized polar group in aryl part generally rendered good inhibitory potentials to these molecules (Figure 5).

Among the following mono-substituted compounds, **8c–f**, a random trend was observed. The molecule **8c** (IC_{50} = 0.3806 ± 0.0103 μM) with a relatively bulky ethyl group at *ortho* position was more active than **8d** (IC_{50} = 2.7219 ± 0.1311 μM) having

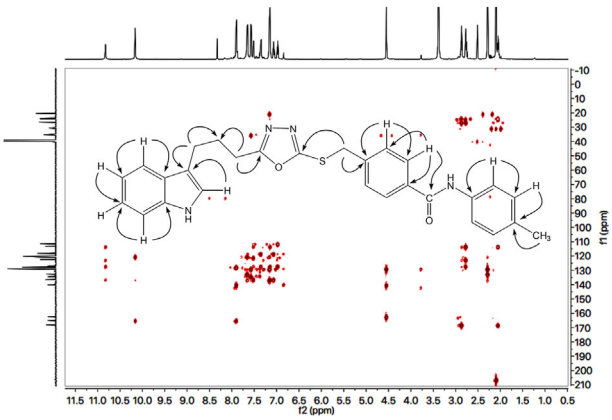

FIGURE 3 HMBC spectrum and significant correlations of **8f** molecule

TABLE 2 Alkaline phosphatase inhibitory and hemolytic activity of bi-heterocyclic benzamides (**8a–k**)

Compounds	Aryl part	Alkaline phosphatase activity IC_{50} ± SEM (μM)	Hemolysis (%) (mean ± SEM)
8a	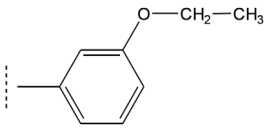	0.0676 ± 0.0057	10.36 ± 0.03
8b	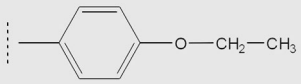	0.0427 ± 0.0167	3.20 ± 0.01
8c	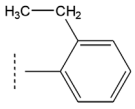	0.3806 ± 0.0103	6.85 ± 0.02
8d	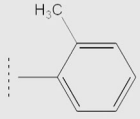	2.7219 ± 0.1311	7.23 ± 0.03
8e	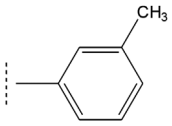	0.9666 ± 0.0427	5.54 ± 0.03
8f	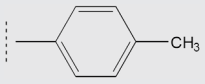	2.8069 ± 0.6172	8.61 ± 0.01
8g	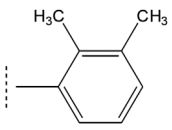	0.0520 ± 0.0011	1.13 ± 0.01
8h	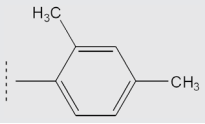	0.4785 ± 0.0497	11.90 ± 0.04
8i	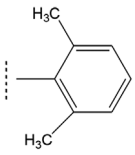	0.3205 ± 0.0431	8.02 ± 0.02
8j	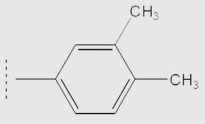	0.2063 ± 0.0111	3.41 ± 0.02
8k	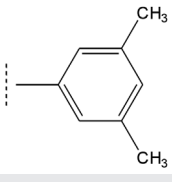	0.0456 ± 0.0048	2.45 ± 0.03
KH_2PO_4		5.2421 ± 0.4722	–
Triton X		–	95.32 ± 0.01

SEM, standard error of the mean; values are expressed in mean ± SEM. PBS hemolysis = 2.45 ± 0.01%.

a smaller methyl group at the same position. Interestingly, **8f** (IC_{50} = 2.8069 ± 0.6172 μM) having the same methyl group but at *para* position showed very resembling activity to that of **8d**. However, **8e** (IC_{50} = 0.9666 ± 0.0427 μM) bearing a *meta*-methyl group behaved as a better inhibitor relative to other two methylated molecules, **8d** and **8f**. It indicated that an electron donating medium-sized group either at *ortho* position or a small group at *meta* position could be considered as creditable options for the better inhibitory potential (Figure 6).

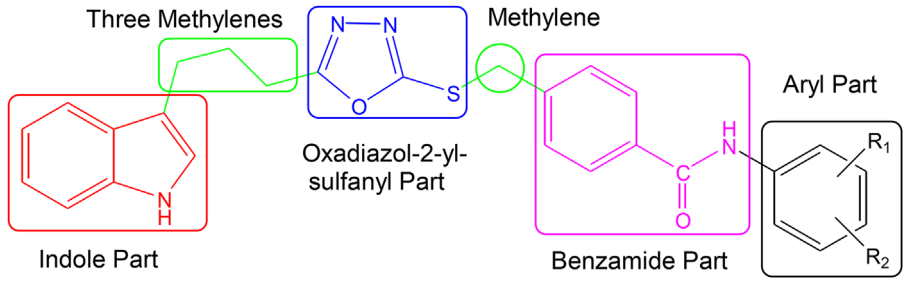

FIGURE 4 General structural features of compounds **8a–k**

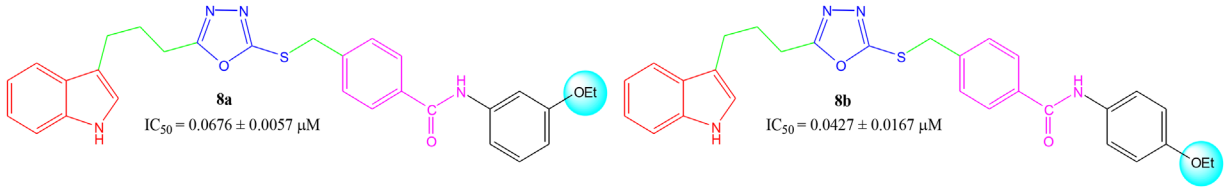

FIGURE 5 Structure–activity relationship of compounds **8a** and **8b**

When the inhibitory potential of following di-methylated regio-isomers was compared, it was observed that the compound **8g** having methyl groups at *ortho* and *meta* positions possessed superior inhibitory activity (IC_{50} = 0.0520 ± 0.0011 μM) as compared to **8h** (IC_{50} = 0.4785 ± 0.0497 μM) and **8i** (IC_{50} = 0.3205 ± 0.0431 μM). In **8h**, these methyl groups were attached at *ortho* and *para* positions while in **8i** a *di-ortho* substitution was present. It indicated that the molecule bearing *ortho* and *meta* methyl groups had better interactions with the enzyme relative to other analogues (Figure 7).

The comparison of **8j**, having *meta* and *para* methyl groups in aryl part, with **8k**, bearing *di-meta* methyl groups, indicated that the latter molecule exhibited enhanced inhibitory potential (IC_{50} = 0.0456 ± 0.0048 μM) relative to former (IC_{50} = 0.2063 ± 0.0111 μM). Here, coherently again the molecule with *meta* substitutions possessed commendable inhibitory activity and was recognized as the second most active compound in the synthetic series (Figure 8).

So, it was inferred from the SAR that among such hybrid bi-heterocycles, the molecules possessing medium-sized polar group at *meta* or *para* position in aryl part, have superb activity. In addition, the presence of at least one small-sized methyl group at *meta* position is another creditable option for the promising inhibitory potential of these molecules.

2.3 | Kinetic mechanism

Presently, the most potent compound **8b** was studied for the mode of inhibition against alkaline phosphatase. The potential of the compound to inhibit the free enzyme and enzyme–substrate complex was determined in terms of EI and ESI constants, respectively, at 37°C. The kinetic studies of the enzyme by the Lineweaver–Burk plot of 1/*V* versus substrate *para*-nitrophenyl phosphate disodium salt 1/[*S*] in the presence of different inhibitor concentrations gave a series of straight lines as shown in Figure 9a. The results of compound **8b** showed that compound intersected within the second quadrant. The analysis showed that V_{max} decreased to new increasing doses of inhibitors on the other hand K_m remained the same. This behavior indicated that **8b**

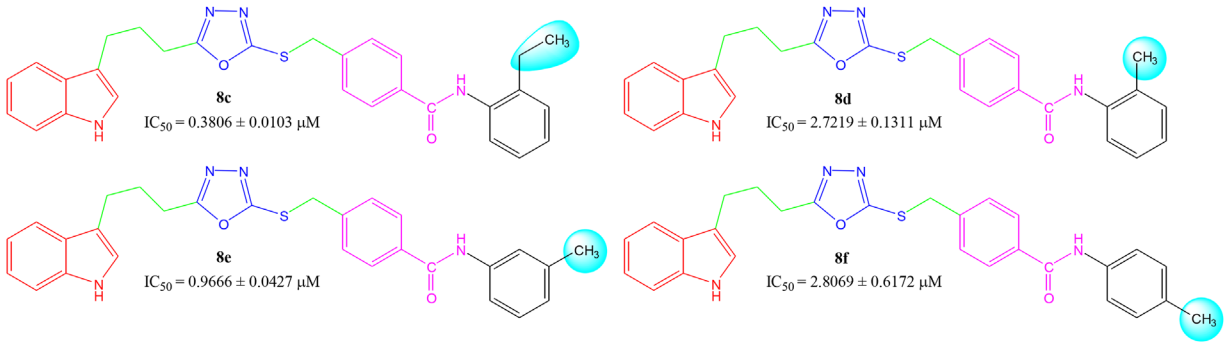

FIGURE 6 Structure–activity relationships of **8c–f**

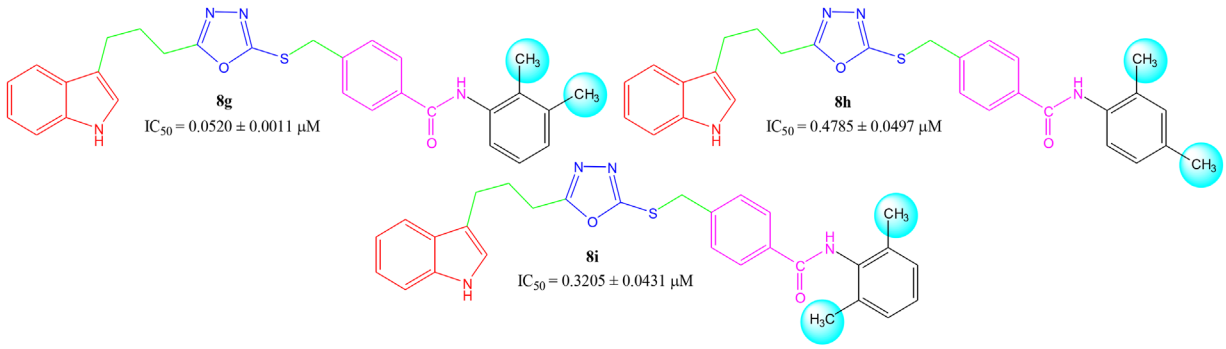

FIGURE 7 Structure–activity relationships of **8g–i**

inhibited the alkaline phosphatase non-competitively to form an enzyme inhibitor complex. Secondary plot of slope against the concentration of inhibitors (Figure 9b) showed enzyme-inhibitor dissociation constant (K_i). The kinetic results are presented in Table 3.

2.4 | Hemolytic activity

All the synthesized compounds, **8a–k**, were also subjected to hemolytic assay to find out their cytotoxicity profile. Results of percentage hemolysis (%) are shown in Table 2. Our results showed that all compounds of this series possessed moderate toxicity toward red blood cell membrane. Maximum membrane toxicity was shown by the compound **8h** (11.90 ± 0.04%) while minimum toxicity was recorded in **8g** (1.13 ± 0.01%). Precisely, a low toxicity was observed for molecule **8k** (2.45 ± 0.03%), **8b** (3.20 ± 0.01%), and **8j** (3.41 ± 0.02%) relative to Triton-X having % hemolysis of 89.11 ± 0.01.

2.5 | Docking energy and binding interaction pattern of synthesized compounds

Molecular docking experiment is best approach to study the binding conformation of ligands within the active region of target proteins.[22–25] To predict the best-fitted conformational position, the synthesized compounds, **8a–k**, were docked against alkaline phosphatase. The generated docked-complexes were examined on the basis of Glide docking score (kcal/mol) and bonding interaction (hydrogen/hydrophobic) pattern. The binding energy values depicted the conformational positions of ligands within the active region of target protein. Results showed that **8c**, **8d**, and **8f** possessed low and good energy values (−4.03, −4.30, and −4.17 kcal/mol), respectively, compared to other designed ligands. Anyhow, among all docking energy values, no big differences were observed because all compounds have similar chemical skeletons except variation in aryl part. The docking energy values are represented in Figure 10.

2.5.1 | Binding pocket and hydrogen binding analysis

Docking analysis showed that all compounds were confined in the active binding region of receptor molecule with different conformational poses. However, the binding of ligands showed their good interactive behavior within the active region of target protein. The binding pocket in surface format and all ligands attachment within active region are depicted in Figure 11(A and B, respectively).

Based on *in vitro* analysis, **8b** was selected to observe the detail binding interactive behavior within the active region of target protein. In alkaline phosphatase docking results, single hydrogen bond was observed in **8b**–receptor docking complex. The oxygen molecule of benzamide interacted with Arg150 with binding distance 1.91 Å. The detail structural analysis reports showed that Arg150 is a part of core region of alkaline phosphatase.[26] The 3D and 2D graphical representation of docking complexes are mentioned in Figures 12 and 13, respectively. Our docking results showed a good correlation with already published data.[27] All the docking-complexes graphical 2D representations are mentioned in supplementary data (Supporting Information Figures S1–S10).

3 | CONCLUSION

In conclusion, the newly synthesized bi-heterocyclic benzamides behaved as promising inhibitors for the calf intestinal alkaline

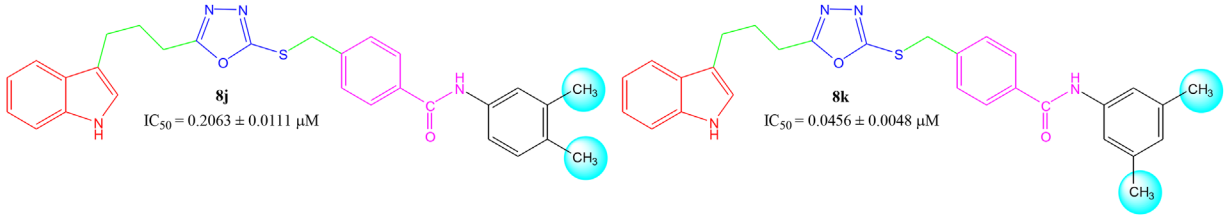

FIGURE 8 Structure–activity relationship of **8j** and **8k**

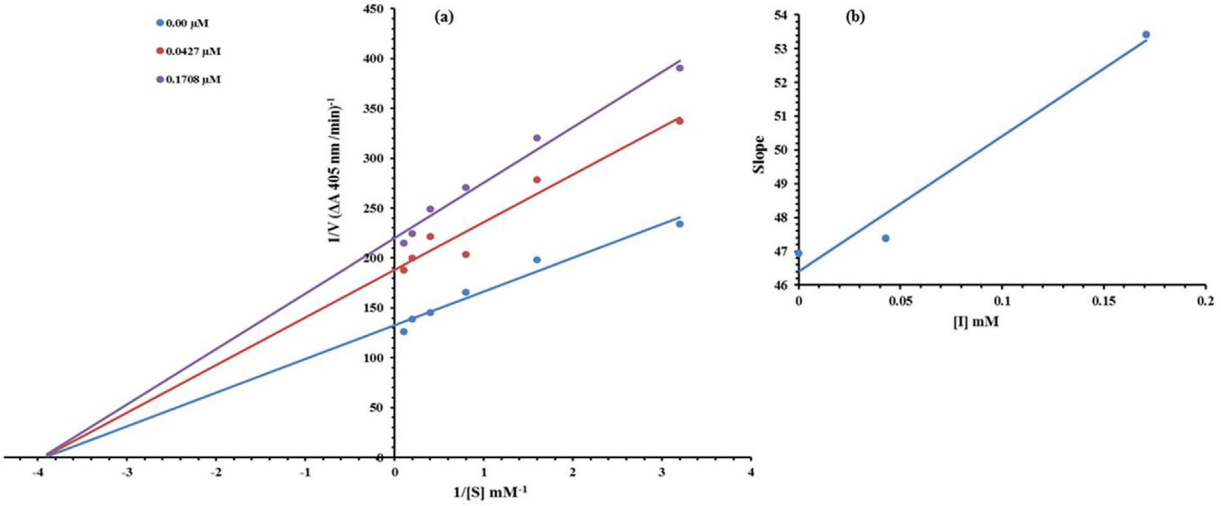

FIGURE 9 Lineweaver–Burk plots for inhibition of alkaline phosphatase in the presence of compound **8b**. (a) Concentrations of **8b** were 0.00, 0.0427, and 0.1708 µM. (b) The inset represents the plot of the slope versus inhibitor **8b** concentrations to determine inhibition constant. The lines were drawn using linear least squares fit

phosphatase. The structural corroboration of compounds **8a–k** was performed through spectroscopic and elemental analysis. Among these derivatives, the molecule **8b**, bearing 4-ethoxy group in aryl part, was identified as the most potent derivative in the series with IC_{50} value of 0.0427 ± 0.0167 µM. Lineweaver–Burk plot showed that **8b** inhibited alkaline phosphatase non-competitively and possessed K_i value of 1.15 µM. The binding profile of **8b** also showed its good interactive behavior within the active region of target protein. So, it was inferred from the current study that **8b** might find its utility as an impressive therapeutic agent for alkaline phosphatase-associated disorders, particularly, normal calcification of bones and teeth.

4 | EXPERIMENTAL

4.1 | Chemistry

4.1.1 | General

Chemicals were purchased from Sigma–Aldrich & Alfa Aesar (Germany) and solvents of analytical grades were supplied by local suppliers. By using open capillary tube method, melting points were taken on Griffin and George apparatus and were uncorrected. By using thin layer chromatography (with ethyl acetate and *n*-hexane (30:70) as mobile phase), initial purity of compounds was detected at 254 nm. Elemental analyses were performed on a Foss Heraeus CHN-O-Rapid instrument and were within ±0.4% of the theoretical values. IR peaks were recorded on a Jasco-320-A spectrometer by using KBr pellet method. EI-MS spectra were measured on a JEOL JMS-600H instrument with data processing system. ^{1}H NMR spectra (δ, ppm) were recorded at 600 MHz (^{13}C NMR spectra, at 150 MHz) in DMSO-d_6 using the Bruker Advance III 600 As-cend spectrometer using BBO probe. The abbreviations used in interpretation of ^{1}H NMR spectra are as follows: s, singlet; d, doublet; dd, doublet of doublets; t, triplet; br.t, broad triplet; q, quartet; quint., quintet; m, multiplet; dist., distorted.

The InChI codes of the investigated compounds together with some biological activity data are provided as Supporting Information.

4.1.2 | Synthesis of ethyl 4-(1*H*-indol-3-yl)butanoate (2)

4-(1*H*-Indol-3-yl)butanoic acid (0.2 mol; **1**) dissolved in absolute ethanol (70 mL) and catalytic amount of concentrated sulfuric acid (20 mL) was taken in a 500 mL round-bottomed (RB) flask and refluxed for 8 h until the maximum completion of reaction, supervised through TLC. At the end, reaction mixture was neutralized with 10% aqueous sodium carbonate (40 mL). The product was isolated by solvent

TABLE 3 Kinetic parameters of the alkaline phosphatase for *para*-nitrophenylphosphate disodium salt activity in the presence of different concentrations of **8b**

Conc. (µM)	V_{max} (Δ*A*/min)	K_m (mM)	Inhibition type	K_i (µM)
0.00	0.007917273	0.25	Non-competitive	1.15
0.0427	0.00532	0.25		
0.1708	0.004646364	0.25		

V_{max}, the reaction velocity; K_m, Michaelis-Menten constant; K_i, EI dissociation constant.

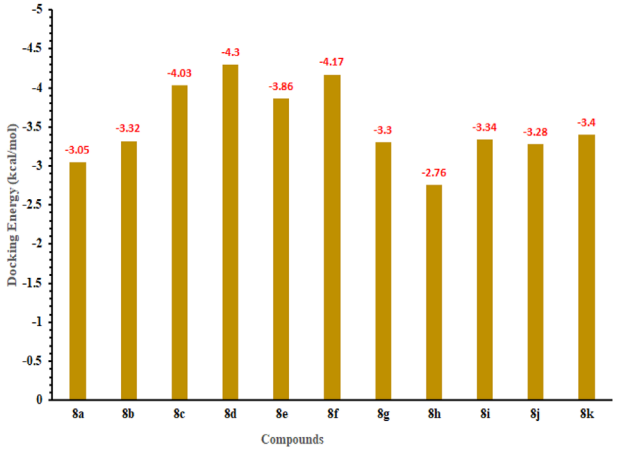

FIGURE 10 Docking energy graph

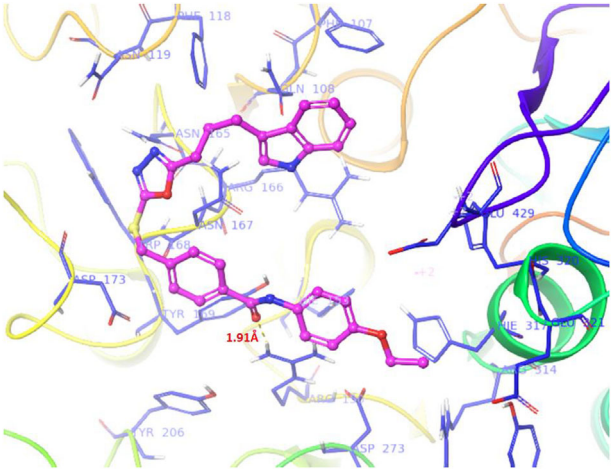

FIGURE 12 The 3D interactions depiction of **8b** against alkaline phosphatase

extraction using chloroform (50 mL × 3). The solvent was distilled off and the required ester, **2**, was obtained as reddish brown liquid.[19,20]

4.1.3 | Synthesis of 4-(1*H*-indol-3-yl)butanohydrazide (3)

4-(1*H*-Indol-3-yl)butanoate (0.15 mol; **2**) in 60 mL methanol and hydrazine monohydrate (80%; 25 mL) was taken in a 500 mL round-bottomed flask. The reaction mixture was refluxed for 14 h at room temperature (RT). After absolute conversion, the acid hydrazide was obtained by distilling methanol off from the reaction mixture. The precipitates were filtered, washed with cold *n*-hexane, and air-dried to get pure 4-(1*H*-indol-3-yl)butanohydrazide (**3**).[19,20]

4.1.4 | Synthesis of 5-[3-(1*H*-indol-3-yl)propyl]-1,3,4-oxadiazol-2-ylhydrosulfide (4)

4-(1*H*-Indol-3-yl)butanohydrazide (0.13 mol; **3**) in absolute ethanol (30 mL) and KOH (0.13 mol) was taken in a RB flask. Carbon disulfide (0.26 mol) was added subsequently. Mixture was refluxed for 16 h. On completion of the reaction, excess chilled distilled water and dil. HCl was added to adjust the pH at 5–6. The precipitates were filtered, washed, and dried to get desired cyclized bi-heterocyclic product, **4**.[19,20]

4.1.5 | Preparation of 4-(chloromethyl)-*N*-(substituted-phenyl)benzamides (7a–k)

Preparation of various 4-(chloromethyl)-*N*-(substituted-phenyl)benzamides (**7a–k**) was carried out by reaction of various substituted anilines (**5a–k**) with 4-(chloromethyl)benzoyl chloride (**6**) in equimolar quantities (0.001 moles) and shaking manually in 10% aqueous Na_2CO_3 solution. Solid precipitates were formed after 20–30 min, which were filtered and washed with cold-distilled water to obtain the desired electrophiles, **7a–k**.[21]

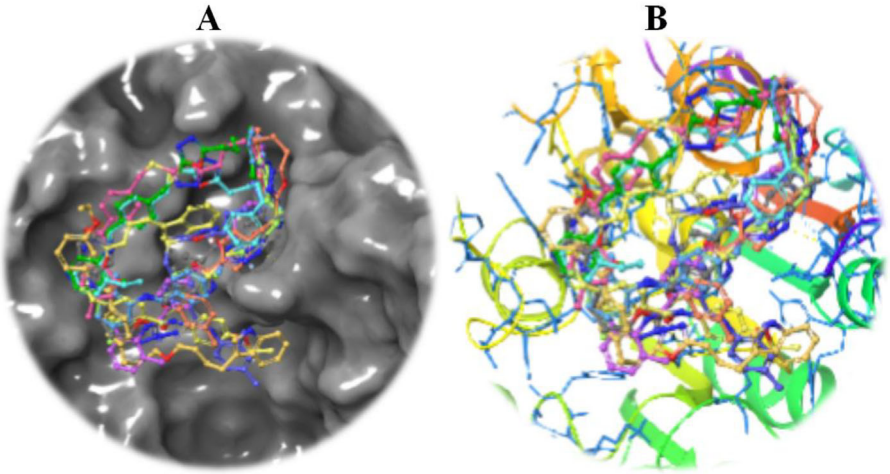

FIGURE 11 (A and B) The binding conformational poses of bi-heterocyclic benzamides within active region of alkaline phosphatase in surface and ribbon format, respectively.

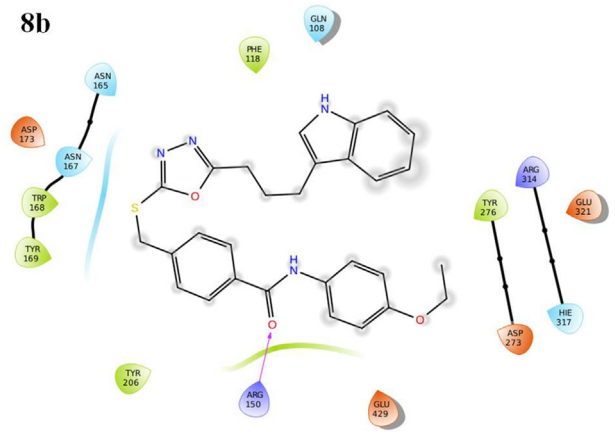

FIGURE 13 The 2D interactions depiction of **8b** against alkaline phosphatase

4.1.6 | Synthesis of 3-[({5-[3-(1*H*-indol-3-yl)propyl]-1,3,4-oxadiazol-2-yl}sulfanyl)methyl]-*N*-(substituted-phenyl)benzamides (8a–k)

Synthesis of 5-[3-(1*H*-indol-3-yl)propyl]-1,3,4-oxadiazol-2-ylhydrosulfide (0.2 g, **4**) was added in DMF (5 mL) contained in a 250 mL round bottom flask at room temperature, added one pinch of LiH and stirred for 30 min. 4-(Chloromethyl)-*N*-(substituted-phenyl)benzamides (**7a–k**) were added in equimolar amounts separately in each respective reaction and stirred for 40–50 h. The completion of the reaction was monitored by TLC and after its completion, the reaction mixture was quenched with ice cold water (100 mL). The respective derivatives, (**8a–k**), were collected through filtration or solvent extraction according to nature of the product.

N-(3-Ethoxyphenyl)-4-[({5-[3-(1*H*-indol-3-yl)propyl]-1,3,4-oxadiazol-2-yl}sulfanyl)methyl]benzamide (8a)

Yellow-colored amorphous powder; yield: 73%; mp: 129°C; mol. formula: $C_{29}H_{28}N_4SO_3$; mol. weight: 512 g/mol; IR (KBr, υ, cm^{-1}): 3290 (N-H str.), 2966 (C-H aromatic str.), 1644 (C═O str.), 1596 (CC aromatic str.), 1525, 1488, 1445 (str. for oxadiazole), 1152 (C-O-C str.), 1125 (C═N str.), 688 (C-S str.); ^{1}H NMR (600 MHz, DMSO-d_6, δ, ppm): 10.82 (s, 1H, NH-1), 10.18 (s, 1H, CONH), 7.89 (br.d, *J* = 7.5 Hz, 2H, H-2‴ & H-6‴), 7.57 (br.d, *J* = 7.7 Hz, 2H, H-3‴ & H-5‴), 7.51 (br.d, *J* = 7.8 Hz, 1H, H-7), 7.46 (br.d, *J* = 6.7 Hz, 1H, H-2″″), 7.37 (dist.d, *J* = 7.5 Hz, 2H, H-4 & H-6″″), 7.23 (br.t, *J* = 7.9 Hz, 1H, H-5″″), 7.14 (s, 1H, H-2), 7.06 (br.t, *J* = 7.1 Hz, 1H, H-6), 6.97 (br.t, *J* = 7.1 Hz, 1H, H-5), 6.67 (br.d, *J* = 7.5 Hz, 1H, H-4″″), 4.55 (s, 2H, CH_2-7‴), 4.02 (q, *J* = 6.7 Hz, 2H, $CH_3\underline{CH_2}$O-3″″), 2.88 (t, *J* = 7.1 Hz, 2H, CH_2-1′), 2.77 (t, *J* = 6.9 Hz, 2H, CH_2-3′), 2.04 (quint., *J* = 7.1 Hz, 2H, CH_2-2′), 1.34 (t, *J* = 6.7 Hz, 3H, $\underline{CH_3}CH_2$O-3″″). ^{13}C NMR (150 MHz, DMSO-d_6, δ, ppm): 168.10 (C-5″), 165.14 (C-8‴), 162.28 (C-2″), 158.63 (C-3″″), 140.34 (C-1″″), 140.25 (C-4‴), 136.28 (C-8), 134.29 (C-1‴), 129.31 (C-5″″), 128.91 (C-3‴ & C-5‴), 127.84 (C-2‴ & C-6‴), 127.00 (C-9), 122.49 (C-2), 120.86 (C-6), 118.17 (C-7), 118.16 (C-5), 113.21 (C-3), 112.36 (C-6″″), 111.21 (C-4), 109.69 (C-4″″), 106.41 (C-2″″), 62.89 ($CH_3\underline{CH_2}$O-3″″), 35.32 (C-7‴), 26.47 (C-2′), 24.25 (C-1′), 23.80 (C-3′), 14.63 ($\underline{CH_3}CH_2$O-3″″). Anal. calcd. for $C_{29}H_{28}N_4SO_3$ (512.18): C, 67.95; H, 5.51; N, 10.93. Found: C, 67.90; H, 5.45; N, 10.89. EI-MS (*m/z*): 512 $(C_{29}H_{28}N_4SO_3)^{\cdot+}$ $(M)^+$, 369 $(C_{19}H_{19}N_3SO_3)^+$, 287 $(C_{16}H_{16}NO_2S)^+$, 258 $(C_{13}H_{12}N_3SO)^{\cdot+}$, 186 $(C_{12}H_{12}NO)^+$, 184 $(C_{12}H_{12}N_2)^{\cdot+}$, 151 $(C_8H_9NO_2)^+$, 143 $(C_{10}H_9N)^+$, 130 $(C_9H_8N)^+$, 120 $(C_8H_{10}N)^+$, 91 $(C_6H_5N)^+$, 78 $(C_5H_4N)^+$.

N-(4-Ethoxyphenyl)-4-[({5-[3-(1*H*-indol-3-yl)propyl]-1,3,4-oxadiazol-2-yl}sulfanyl)methyl]benzamide (8b)

Light brown-colored sticky liquid; yield: 78%; mol. formula: $C_{29}H_{28}N_4SO_3$; mol. weight: 512 g/mol; IR (KBr, υ, cm^{-1}): 3293 (N-H str.), 2966 (C-H aromatic str.), 1642 (C═O str.), 1598 (C═C aromatic str.), 1529, 1488, 1447 (str. for oxadiazole), 1153 (C-O-C str.), 1126 (C═N str.), 687 (C-S str.); ^{1}H NMR (600 MHz, DMSO-d_6, δ, ppm): 10.81 (s, 1H, NH-1), 9.92 (s, 1H, CONH), 7.81 (br.d, *J* = 7.8 Hz, 2H, H-2‴ & H-6‴), 7.57 (br.d, *J* = 7.8 Hz, 2H, H-3‴ & H-5‴), 7.51 (br.s, 1H, H-7), 7.41 (br.d, *J* = 7.8 Hz, 2H, H-2″″ & H-6″″), 7.35 (m, 1H, H-4), 7.14 (br.s, 1H, H-2), 7.07 (br.t, *J* = 7.8 Hz, 1H, H-6), 6.97 (br.t, *J* = 7.8 Hz, 1H, H-5), 6.84 (br.s, 2H, H-3″″ & H-5″″), 4.55 (s, 2H, CH_2-7‴), 3.86 (s, 2H, $CH_3\underline{CH_2}$O-4″″), 2.87 (t, *J* = 7.2 Hz, 2H, CH_2-1′), 2.75 (t, *J* = 7.1 Hz, 2H, CH_2-3′), 2.06–2.04 (m, 2H, CH_2-2′), 1.16–1.10 (m, 3H, $\underline{CH_3}CH_2$O-4″″). ^{13}C NMR (150 MHz, DMSO-d_6, δ, ppm): 168.10 (C-5″), 165.13 (C-8‴), 162.29 (C-2″), 140.29 (C-4‴), 139.81 (C-4″″), 136.28 (C-8), 133.53 (C-1‴), 130.69 (C-1″″), 128.52 (C-3‴ & C-5‴), 128.09 (C-2″″ & C-6″″), 127.76 (C-2‴ & C-6‴), 126.99 (C-9), 126.58 (C-3″″ & C-5″″), 122.50 (C-2), 120.86 (C-6), 118.17 (C-5 & C-7), 113.21 (C-3), 111.34 (C-4), 63.06 ($CH_3\underline{CH_2}$O-4″″), 35.32 (C-7‴), 26.47 (C-2′), 24.25 (C-1′), 23.79 (C-3′), 14.10 ($\underline{CH_3}CH_2$O-4″″); Anal. calcd. for $C_{29}H_{28}N_4SO_3$ (512.18): C, 67.95; H, 5.51; N, 10.93. Found: C, 67.90; H, 5.45; N, 10.89. EI-MS (*m/z*): 512 $(C_{29}H_{28}N_4SO_3)^{\cdot+}$ $(M)^+$, 369 $(C_{19}H_{19}N_3SO_3)^+$, 287 $(C_{16}H_{16}NO_2S)^+$, 258 $(C_{13}H_{12}N_3SO)^{\cdot+}$, 186 $(C_{12}H_{12}NO)^+$, 184 $(C_{12}H_{12}N_2)^{\cdot+}$, 151 $(C_8H_9NO_2)^+$, 143 $(C_{10}H_9N)^+$, 130 $(C_9H_8N)^+$, 120 $(C_8H_{10}N)^+$, 91 $(C_6H_5N)^+$, 78 $(C_5H_4N)^+$.

N-(2-Ethylphenyl)-4-[({5-[3-(1*H*-indol-3-yl)propyl]-1,3,4-oxadiazol-2-yl}sulfanyl)methyl]benzamide (8c)

Brown-colored amorphous powder; yield: 55%; mp: 140°C; mol. formula: $C_{29}H_{28}N_4SO_2$; mol. weight: 496 g/mol; IR (KBr, υ, cm^{-1}): 3286 (N-H str.), 2957 (C-H aromatic str.), 1656 (CO str.), 1599 (C═C aromatic str.), 1527, 1481, 1441 (str. for oxadiazole), 1141 (C-O-C str.), 1101 (CN str.), 677 (C-S str.); ^{1}H NMR (600 MHz, DMSO-d_6, δ, ppm): 10.82 (s, 1H, NH-1), 9.87 (s, 1H, CONH), 7.93 (br.d, *J* = 7.3 Hz, 2H, H-2‴ & H-6‴), 7.57 (br.d, *J* = 7.3 Hz, 2H, H-3‴ & H-5‴), 7.51 (br.d, *J* = 7.9 Hz, 1H, H-7), 7.34 (br.d, *J* = 7.9 Hz, 1H, H-4), 7.29 (br.d, *J* = 7.2 Hz, 1H, H-6″″), 7.23 (br.d, *J* = 7.3 Hz, 1H, H-3″″), 7.18–7.17 (m, 2H, H-4″″ & H-5″″), 7.14 (br.s, 1H, H-2), 7.06 (br.t, *J* = 6.7 Hz, 1H, H-6), 6.97 (br.t, *J* = 6.9 Hz, 1H, H-5), 4.55 (s, 2H, CH_2-7‴), 2.87 (t, *J* = 6.8 Hz, 2H, CH_2-1′), 2.77 (t, *J* = 6.4 Hz, 2H, CH_2-3′), 2.62 (quartet, *J* = 6.8 Hz, 2H, $CH_3\underline{CH_2}$-2″″), 2.05 (q, *J* = 6.8 Hz, 2H, CH_2-2′), 1.13 (t, *J* = 6.8 Hz, 3H, $\underline{CH_3}CH_2$-2″″). ^{13}C NMR (150 MHz, DMSO-d_6, δ, ppm): 168.11 (C-5″), 165.22 (C-8‴), 162.29 (C-2″), 140.24 (C-4‴), 139.77 (C-1″″), 136.28 (C-8), 135.66 (C-1‴), 133.81 (C-2″″), 128.96 (C-3‴ & C-5‴),

128.55 (C-3‴), 127.78 (C-2‴ & C-6‴), 127.55 (C-4‴), 127.00 (C-9), 126.46 (C-5‴), 125.96 (C-6‴), 122.50 (C-2), 120.86 (C-6), 118.18 (C-7), 118.16 (C-5), 113.21 (C-3), 111.35 (C-4), 35.32 (C-7‴), 26.47 (C-2′), 24.25 (C-1′), 23.79 (C-3′), 23.92 (CH_3 $\underline{CH_2}$-2‴), 14.08 ($\underline{CH_3}CH_2$-2‴). Anal. calcd. for $C_{29}H_{28}N_4SO_2$ (496.19): C, 69.69; H, 5.43; N, 11.61. Found: C, 69.67; H, 5.45; N, 11.58. EI-MS (*m/z*): 496 $(C_{29}H_{28}N_4SO_2)^{\cdot+}$ $(M)^+$, 339 $(C_{18}H_{17}N_3SO_2)^+$, 258 $(C_{13}H_{12}N_3SO)^{\cdot+}$, 224 $(C_{15}H_{14}NO)^+$, 186 $(C_{12}H_{12}NO)^+$, 184 $(C_{12}H_{12}N_2)^{\cdot+}$, 143 $(C_{10}H_9N)^+$, 130 $(C_9H_8N)^+$, 120 $(C_8H_{10}N)^+$, 91 $(C_6H_5N)^+$, 78 $(C_5H_4N)^+$.

4-[({5-[3-(1*H*-Indol-3-yl)propyl]-1,3,4-oxadiazol-2-yl}sulfanyl)-methyl]-*N*-(2-methylphenyl)benzamide (8d)

Light brown-colored amorphous powder; yield: 63%; mp: 211°C; mol. formula: $C_{28}H_{26}N_4SO_2$; mol. weight: 482 g/mol; IR (KBr, υ, cm^{-1}): 3296 (N-H str.), 2958 (C-H aromatic str.), 1652 (C═O str.), 1591 (CC aromatic str.), 1531, 1489, 1444 (str. for oxadiazole), 1155 (C-O-C str.), 1122 (CN str.), 687 (C-S str.); ^{1}H NMR (600 MHz, DMSO-d_6, δ, ppm): 10.81 (s, 1H, NH-1), 9.86 (s, 1H, CONH), 7.93 (br.d, *J* = 7.5 Hz, 2H, H-2‴ & H-6‴), 7.57 (br.d, *J* = 7.7 Hz, 2H, H-3‴ & H-5‴), 7.51 (br.d, *J* = 7.9 Hz, 1H, H-7), 7.37 (br.d, *J* = 7.4 Hz, 1H, H-6‴), 7.33 (m, 1H, H-4), 7.27 (br.d, *J* = 7.4 Hz, 1H, H-3‴), 7.21 (br.t, *J* = 7.5 Hz, 1H, H-5‴), 7.17 (br.t, *J* = 7.5 Hz, 1H, H-4‴), 7.14 (br.s, 1H, H-2), 7.06 (br.t, *J* = 7.2 Hz, 1H, H-6), 6.97 (br.t, *J* = 7.1 Hz, 1H, H-5), 4.55 (s, 2H, CH_2-7‴), 2.87 (t, *J* = 7.2 Hz, 2H, CH_2-1′), 2.76 (t, *J* = 7.2 Hz, 2H, CH_2-3′), 2.14 (s, 3H, CH_3-2‴), 2.04 (quint., *J* = 7.3 Hz, 2H, CH_2-2′). ^{13}C NMR (150 MHz, DMSO-d_6, δ, ppm): 168.10 (C-5″), 164.85 (C-8‴), 162.38 (C-2″), 140.31 (C-4‴), 136.27 (C-8), 135.69 (C-1‴), 134.21 (C-1‴), 130.63 (C-2‴), 130.25 (C-3‴), 128.95 (C-3‴ & C-5‴), 127.82 (C-2‴ & C-6‴), 126.98 (C-9), 126.50 (C-6‴), 125.94 (C-4‴ & C-5‴), 122.50 (C-2), 120.86 (C-6), 118.17 (C-5 & C-7), 113.23 (C-3), 111.34 (C-4), 35.32 (C-7‴), 26.47 (C-2′), 24.49 (C-1′), 23.79 (C-3′), 17.84 (CH_3-2‴). Anal. calcd. for $C_{28}H_{26}N_4SO_2$ (482.18): C, 69.69; H, 5.43; N, 11.61. Found: C, 69.67; H, 5.45; N, 11.58. EI-MS (*m/z*): 482 $(C_{28}H_{26}N_4SO_2)^{\cdot+}$ $(M)^+$, 339 $(C_{18}H_{17}N_3SO_2)^+$, 258 $(C_{13}H_{12}N_3SO)^{\cdot+}$, 224 $(C_{15}H_{14}NO)^+$, 186 $(C_{12}H_{12}NO)^+$, 184 $(C_{12}H_{12}N_2)^{\cdot+}$, 143 $(C_{10}H_9N)^+$, 130 $(C_9H_8N)^+$, 120 $(C_8H_{10}N)^+$, 91 $(C_6H_5N)^+$, 78 $(C_5H_4N)^+$.

4-[({5-[3-(1*H*-Indol-3-yl)propyl]-1,3,4-oxadiazol-2-yl}sulfanyl)-methyl]-*N*-(3-methylphenyl)benzamide (8e)

Camel brown-colored amorphous powder; yield: 61%; mp: 106°C; mol. formula: $C_{28}H_{26}N_4SO_2$; mol. weight: 482 g/mol; IR (KBr, υ, cm^{-1}): 3274 (N-H str.), 2953 (C-H aromatic str.), 1703 (C═O str.), 1590 (CC aromatic str.), 1531, 1489, 1452 (str. for oxadiazole), 1159 (C-O-C str.), 1100 (C═N str.), 666 (C-S str.); ^{1}H NMR (600 MHz, DMSO-d_6, δ, ppm): 10.81 (s, 1H, NH-1), 10.15 (s, 1H, CONH), 7.90 (br.d, *J* = 7.5 Hz, 2H, H-2‴ & H-6‴), 7.64 (br.s, 1H, H-2‴), 7.58 (dist.d, *J* = 7.9 Hz, 3H, H-3‴, H-5‴ & H-6‴), 7.51 (br.d, *J* = 7.9 Hz, 1H, H-7), 7.34 (br.d, *J* = 7.8 Hz, 1H, H-4), 7.23 (br.t, *J* = 7.8 Hz, 1H, H-5‴), 7.14 (s, 1H, H-2), 7.06 (br.t, *J* = 7.4 Hz, 1H, H-6), 6.97 (br.t, *J* = 7.1 Hz, 1H, H-5), 6.93 (br.d, *J* = 7.3 Hz, 1H, H-4‴), 4.54 (s, 2H, CH_2-7‴), 2.88 (t, *J* = 7.2 Hz, 2H, CH_2-1′), 2.76 (t, *J* = 7.20 Hz, 2H, CH_2-3′), 2.31 (s, 3H, CH_3-3‴), 2.09–2.03 (m, 2H, CH_2-2′). ^{13}C NMR (150 MHz, DMSO-d_6, δ, ppm): 168.10 (C-5″), 164.85 (C-8‴), 162.28 (C-2″), 140.27 (C-4‴), 138.98 (C-1‴), 137.69 (C-3‴), 136.28 (C-8), 134.30 (C-1‴), 128.90 (C-3‴ & C-5‴), 128.14 (C-5‴), 127.82 (C-2‴ & C-6‴), 126.99 (C-9), 124.32 (C-4‴), 122.49 (C-2), 120.91 (C-2‴), 120.86 (C-6), 118.17 (C-7), 118.16 (C-5), 117.48 (C-6‴), 113.21 (C-3), 111.34 (C-4), 35.33 (C-7‴), 26.47 (C-2′), 24.25 (C-1′), 23.80 (C-3′), 21.17 (CH_3-3‴). Anal. calcd. for $C_{28}H_{26}N_4SO_2$ (482.18): C, 69.69; H, 5.43; N, 11.61. Found: C, 69.67; H, 5.45; N, 11.58. EI-MS (*m/z*): 482 $(C_{28}H_{26}N_4SO_2)^{\cdot+}$ $(M)^+$, 339 $(C_{18}H_{17}N_3SO_2)^+$, 258 $(C_{13}H_{12}N_3SO)^{\cdot+}$, 224 $(C_{15}H_{14}NO)^+$, 186 $(C_{12}H_{12}NO)^+$, 184 $(C_{12}H_{12}N_2)^{\cdot+}$, 143 $(C_{10}H_9N)^+$, 130 $(C_9H_8N)^+$, 120 $(C_8H_{10}N)^+$, 91 $(C_6H_5N)^+$, 78 $(C_5H_4N)^+$.

4-[({5-[3-(1*H*-Indol-3-yl)propyl]-1,3,4-oxadiazol-2-yl}sulfanyl)-methyl]-*N*-(4-methylphenyl)benzamide (8f)

Yellow-colored amorphous powder; yield: 87%; mp: 168°C; mol. formula: $C_{28}H_{26}N_4SO_2$; mol. weight: 482 g/mol; IR (KBr, υ, cm^{-1}): 3317 (N-H str.), 2955 (C-H aromatic str.), 1654 (CO str.), 1599 (C═C aromatic str.), 1535, 1484, 1449 (str. for oxadiazole), 1155 (C-O-C str.), 1103 (CN str.), 681 (C-S str.); ^{1}H NMR (600 MHz, DMSO-d_6, δ, ppm): 10.82 (s, 1H, NH-1), 10.16 (s, 1H, CONH), 7.91 (br.d, *J* = 7.9 Hz, 2H, H-2‴ & H-6‴), 7.65 (br.d, *J* = 7.9 Hz, 2H, H-3‴ & H-5‴), 7.57 (br.d, *J* = 7.8 Hz, 2H, H-3‴ & H-5‴), 7.51 (br.d, *J* = 7.6 Hz, 1H, H-7), 7.35 (br.d, *J* = 8.0 Hz, 1H, H-4), 7.16–7.14 (m, 3H, H-2, H-2‴ & H-6‴), 7.06 (br.t, *J* = 7.2 Hz, 1H, H-6), 6.97 (br.t, *J* = 7.2 Hz, 1H, H-5), 4.54 (s, 2H, CH_2-7‴), 2.86 (t, *J* = 7.2 Hz, 2H, CH_2-1′), 2.77 (t, *J* = 7.1 Hz, 2H, CH_2-3′), 2.09 (s, 3H, CH_3-4‴), 2.05 (quint., *J* = 7.2 Hz, 2H, CH_2-2′). ^{13}C NMR (150 MHz, DMSO-d_6, δ, ppm): 168.09 (C-5″), 164.90 (C-8‴), 162.29 (C-2″), 140.19 (C-4‴), 136.56 (C-1‴), 136.29 (C-8), 134.35 (C-1‴), 132.57 (C-4‴), 128.93 (C-3‴ & C-5‴), 128.88 (C-2‴ & C-6‴), 127.80 (C-2‴ & C-6‴), 127.00 (C-9), 122.49 (C-2), 120.86 (C-6), 120.31 (C-3‴ & C-5‴), 118.18 (C-7), 118.16 (C-5), 113.22 (C-3), 111.35 (C-4), 35.34 (C-7‴), 26.48 (C-2′), 24.26 (C-1′), 23.81 (C-3′), 20.46 (CH_3-4‴). Anal. calcd. for $C_{28}H_{26}N_4SO_2$ (482.18): C, 69.69; H, 5.43; N, 11.61. Found: C, 69.67; H, 5.45; N, 11.58. EI-MS (*m/z*): 482 $(C_{28}H_{26}N_4SO_2)^{\cdot+}$ $(M)^+$, 339 $(C_{18}H_{17}N_3SO_2)^+$, 258 $(C_{13}H_{12}N_3SO)^{\cdot+}$, 224 $(C_{15}H_{14}NO)^+$, 186 $(C_{12}H_{12}NO)^+$, 184 $(C_{12}H_{12}N_2)^{\cdot+}$, 143 $(C_{10}H_9N)^+$, 130 $(C_9H_8N)^+$, 120 $(C_8H_{10}N)^+$, 91 $(C_6H_5N)^+$, 78 $(C_5H_4N)^+$.

N-(2,3-Dimethylphenyl)-4-[({5-[3-(1*H*-indol-3-yl)propyl]-1,3,4-oxadiazol-2-yl}sulfanyl)methyl]benzamide (8g)

Light yellow-colored amorphous powder; yield: 89%; mp: 138°C; mol. formula: $C_{29}H_{28}N_4SO_2$; mol. weight: 496 g/mol; IR (KBr, cm^{-1}): υ 3286 (N-H str.), 2957 (C-H aromatic str.), 1656 (C═O str.), 1599 (C═C aromatic str.), 1527, 1481, 1441 (str. for oxadiazole), 1141 (C-O-C str.), 1101 (C═N str.), 677 (C-S str.); ^{1}H NMR (600 MHz, DMSO-d_6, δ, ppm): 10.82 (s, 1H, NH-1), 9.92 (s, 1H, CONH), 7.94 (br.dd, *J* = 7.6, 11.4 Hz, 2H, H-2‴ & H-6‴), 7.57 (br.d, *J* = 7.8 Hz, 2H, H-3‴ & H-5‴), 7.51 (br.d, *J* = 7.8 Hz, 1H, H-7), 7.33 (br.d, *J* = 7.9 Hz, 1H, H-4), 7.14 (br.s, 1H, H-2), 7.11–7.05 (m, 4H, H-6, H-4‴, H-5‴ & H-6‴), 6.97 (br.t, *J* = 7.4 Hz, 1H, H-5), 4.55 (s, 2H, CH_2-7‴), 2.87 (t, *J* = 7.3 Hz, 2H, CH_2-1′), 2.76 (t, *J* = 7.2 Hz, 2H, CH_2-3′), 2.28 (s, 3H, CH_3-3‴), 2.11–2.03 (m, 5H, CH_2-2′ & CH_3-2‴). ^{13}C NMR (150 MHz, DMSO-d_6, δ, ppm): 168.10 (C-5″), 164.89 (C-8‴), 162.29 (C-2″), 140.24 (C-4‴), 136.92 (C-3‴), 136.28 (C-8), 136.16 (C-1‴), 133.86 (C-1‴), 132.66 (C-2‴), 128.93 (C-3‴ &

C-5‴), 127.80 (C-2‴ & C-6‴), 127.50 (C-4‴′), 127.00 (C-9), 125.19 (C-5‴′), 124.63 (C-6‴′), 122.50 (C-2), 120.86 (C-6), 118.18 (C-7), 118.16 (C-5), 113.20 (C-3), 111.35 (C-4), 35.33 (C-7‴), 26.47 (C-2′), 24.25 (C-1′), 23.80 (C-3′), 20.09 (CH_3-3‴′), 14.16 (CH_3-2‴′). Anal. calcd. for $C_{29}H_{28}N_4SO_2$ (496.19): C, 70.14; H, 5.68; N, 11.28. Found: C, 70.10; H, 5.65; N, 11.22. EI-MS (*m/z*): 496 $(C_{29}H_{28}N_4SO_2)^{\cdot+}$ $(M)^+$, 353 $(C_{19}H_{19}N_3SO_2)^+$, 258 $(C_{13}H_{12}N_3SO)^{\cdot+}$, 239 $(C_{16}H_{17}NO)^+$, 186 $(C_{12}H_{12}NO)^+$, 184 $(C_{12}H_{12}N_2)^{\cdot+}$, 143 $(C_{10}H_9N)^+$, 130 $(C_9H_8N)^+$, 120 $(C_8H_{10}N)^+$, 91 $(C_6H_5N)^+$, 78 $(C_5H_4N)^+$.

N-(2,4-Dimethylphenyl)-4-[({5-[3-(1*H*-indol-3-yl)propyl]-1,3,4-oxadiazol-2-yl}sulfanyl)methyl]benzamide (8h)

Yellow-colored amorphous powder; yield: 93%; mp: 177°C; mol. formula: $C_{29}H_{28}N_4SO_2$; mol. weight: 496 g/mol; IR (KBr, υ, cm^{-1}): 3283 (N-H str.), 2957 (C-H aromatic str.), 1654 (C═O str.), 1598 (C═C aromatic str.), 1526, 1481, 1441 (str. for oxadiazole), 1142 (C-O-C str.), 1100 (C═N str.), 677 (C-S str.); ^{1}H NMR (600 MHz, DMSO-d_6, δ, ppm): 10.81 (s, 1H, NH-1), 9.81 (s, 1H, CONH), 7.92 (dist.d, *J* = 5.8 Hz, 2H, H-2‴ & H-6‴), 7.56 (dist.d, *J* = 6.3 Hz, 2H, H-3‴ & H-5‴), 7.51 (br.d, *J* = 6.7 Hz, 1H, H-7), 7.34 (br.d, *J* = 7.4 Hz, 1H, H-4), 7.17 (br.d, *J* = 6.6 Hz, 1H, H-6‴′), 7.13 (br.s, 1H, H-2), 7.07 (br.s, 2H, H-6 & H-3‴′), 7.01 (br.d, *J* = 6.6 Hz, 1H, H-5‴′), 6.97 (m, 1H, H-5), 4.53 (s, 2H, CH_2-7‴), 2.87 (t, *J* = 7.4 Hz, 2H, CH_2-1′), 2.74 (t, *J* = 7.3 Hz, 2H, CH_2-3′), 2.27 (s, 3H, CH_3-4‴′), 2.17 (s, 3H, CH_3-2‴′), 2.05–2.03 (m, 2H, CH_2-2′). ^{13}C NMR (150 MHz, DMSO-d_6, δ, ppm): 168.13 (C-5″), 164.90 (C-8‴), 162.32 (C-2″), 140.23 (C-4‴), 136.27 (C-8), 135.12 (C-1‴), 133.83 (C-1‴′), 133.63 (C-2‴′), 133.50 (C-4‴′), 130.78 (C-3‴′), 128.92 (C-3‴ & C-5‴), 127.78 (C-2‴ & C-6‴), 126.98 (C-9), 126.47 (C-5‴′ & C-6‴′), 122.48 (C-2), 120.88 (C-6), 118.18 (C-7), 118.17 (C-5), 113.23 (C-3), 111.36 (C-4), 35.33 (C-7‴), 26.45 (C-2′), 24.22 (C-1′), 23.84 (C-3′), 20.48 (CH_3-4‴′), 17.73 (CH_3-2‴′); Anal. calcd. for $C_{29}H_{28}N_4SO_2$ (496.19): C, 70.14; H, 5.68; N, 11.28. Found: C, 70.10; H, 5.65; N, 11.22. EI-MS (*m/z*): 496 $(C_{29}H_{28}N_4SO_2)^{\cdot+}$ $(M)^+$, 353 $(C_{19}H_{19}N_3SO_2)^+$, 258 $(C_{13}H_{12}N_3SO)^{\cdot+}$, 239 $(C_{16}H_{17}NO)^+$, 186 $(C_{12}H_{12}NO)^+$, 184 $(C_{12}H_{12}N_2)^{\cdot+}$, 143 $(C_{10}H_9N)^+$, 130 $(C_9H_8N)^+$, 120 $(C_8H_{10}N)^+$, 91 $(C_6H_5N)^+$, 78 $(C_5H_4N)^+$.

N-(2,6-Dimethylphenyl)-4-[({5-[3-(1*H*-indol-3-yl)propyl]-1,3,4-oxadiazol-2-yl}sulfanyl)methyl]benzamide (8i)

Light yellow-colored amorphous powder; yield: 91%; mp: 102°C; mol. formula: $C_{29}H_{28}N_4SO_2$; mol. weight: 496 g/mol; IR (KBr, υ, cm^{-1}): 3298 (N-H str.), 2961 (C-H aromatic str.), 1653 (CO str.), 1581 (C═C aromatic str.), 1527, 1483, 1441 (str. for oxadiazole), 1157 (C-O-C str.), 1121 (C═N str.), 689 (C-S str.); ^{1}H NMR (600 MHz, DMSO-d_6, δ, ppm): 10.77 (s, 1H, NH-1), 9.80 (s, 1H, CONH), 7.93 (br.d, *J* = 7.6, Hz, 2H, H-2‴ & H-6‴), 7.55 (br.d, *J* = 7.8 Hz, 2H, H-3‴ & H-5‴), 7.49 (br.d, *J* = 7.8 Hz, 1H, H-7), 7.34 (br.d, *J* = 8.0 Hz, 1H, H-4), 7.10 (m, 3H, H-3‴″, H-4‴″ & H-5‴″), 7.13 (br.s, 1H, H-2), 7.06 (br.t, *J* = 7.6 Hz, 1H, H-6), 6.96 (br.t, *J* = 7.7 Hz, 1H, H-5), 4.50 (s, 2H, CH_2-7‴), 2.87 (t, *J* = 7.2 Hz, 2H, CH_2-1′), 2.78 (t, *J* = 7.3 Hz, 2H, CH_2-3′), 2.14 (s, 6H, CH_3-2‴″ & CH_3-6‴″), 2.02 (quint., *J* = 7.3 Hz, 2H, CH_2-2′). ^{13}C NMR (150 MHz, DMSO-d_6, δ, ppm): 168.20 (C-5″), 164.87 (C-8‴), 162.39 (C-2″), 140.31 (C-4‴), 136.25 (C-8), 135.56 (C-2‴″ & C-6‴″), 135.03 (C-1‴), 133.52 (C-1‴″), 129.00 (C-3‴ & C-5‴), 128.00 (C-2‴, C-3‴″, C-5‴″ & C-6‴), 126.75 (C-4‴″), 126.95 (C-9), 122.46 (C-2), 120.92 (C-6), 118.23 (C-7), 118.15 (C-5), 113.24 (C-3), 111.38 (C-4), 35.30 (C-7‴), 26.40 (C-2′), 24.25 (C-1′), 23.77 (C-3′), 17.90 (CH_3-2‴″ & CH_3-6‴″). Anal. calcd. for $C_{29}H_{28}N_4SO_2$ (496.19): C, 70.14; H, 5.68; N, 11.28. Found: C, 70.10; H, 5.65; N, 11.22 EI-MS (*m/z*): 496 $(C_{29}H_{28}N_4SO_2)^{\cdot+}$ $(M)^+$, 353 $(C_{19}H_{19}N_3SO_2)^+$, 258 $(C_{13}H_{12}N_3SO)^{\cdot+}$, 239 $(C_{16}H_{17}NO)^+$, 186 $(C_{12}H_{12}NO)^+$, 184 $(C_{12}H_{12}N_2)^{\cdot+}$, 143 $(C_{10}H_9N)^+$, 130 $(C_9H_8N)^+$, 120 $(C_8H_{10}N)^+$, 91 $(C_6H_5N)^+$, 78 $(C_5H_4N)^+$.

N-(3,4-Dimethylphenyl)-4-[({5-[3-(1*H*-indol-3-yl)propyl]-1,3,4-oxadiazol-2-yl}sulfanyl)methyl]benzamide (8j)

Yellow-colored amorphous powder; yield: 77%; mp: 104°C; mol. formula: $C_{29}H_{28}N_4SO_2$; mol. weight: 496 g/mol; IR (KBr, υ, cm^{-1}): 3292 (N-H str.), 2949 (C-H aromatic str.), 1666 (C═O str.), 1599 (C═C aromatic str.), 1528, 1487, 1449 (str. for oxadiazole), 1159 (C-O-C str.), 1109 (CN str.), 688 (C-S str.); ^{1}H NMR (600 MHz, DMSO-d_6, δ, ppm): 10.81 (s, 1H, NH-1), 10.09 (s, 1H, CONH), 7.95 (br.d, *J* = 7.4 Hz, 2H, H-2‴ & H-6‴), 7.55 (br.d, *J* = 7.4 Hz, 2H, H-3‴ & H-5‴), 7.88 (br.s, 1H, H-2‴″), 7.51 (br.d, *J* = 7.8 Hz, 1H, H-7), 7.48 (br.d, *J* = 7.7 Hz, 1H, H-6‴″), 7.34 (br.d, *J* = 8.1 Hz, 1H, H-4), 7.09 (br.d, *J* = 7.8 Hz, 1H, H-5‴″), 7.13 (br.s, 1H, H-2), 7.06 (br.t, *J* = 7.2 Hz, 1H, H-6), 6.97 (br.t, *J* = 7.2 Hz, 1H, H-5), 4.52 (s, 2H, CH_2-7‴), 2.88 (t, *J* = 7.1 Hz, 2H, CH_2-1′), 2.76 (t, *J* = 7.1 Hz, 2H, CH_2-3′), 2.18 (s, 3H, CH_3-4‴″), 2.08 (s, 3H, CH_3-3‴″), 2.04 (quint., *J* = 7.0 Hz, 2H, CH_2-2′). ^{13}C NMR (150 MHz, DMSO-d_6, δ, ppm): 168.12 (C-5″), 164.85 (C-8‴), 162.31 (C-2″), 140.16 (C-4‴), 136.70 (C-3‴″), 136.27 (C-8), 136.11 (C-1‴″), 134.32 (C-1‴), 131.45 (C-4‴″), 128.87 (C-3‴ & C-5‴), 127.93 (C-2‴ & C-6‴), 126.98 (C-9), 122.48 (C-2), 121.60 (C-5‴″), 120.88 (C-6), 118.18 (C-7), 118.04 (C-5), 117.96 (C-2‴″), 117.91 (C-6‴″), 113.23 (C-3), 111.35 (C-4), 35.34 (C-7‴), 26.45 (C-2′), 24.22 (C-1′), 23.77 (C-3′), 19.57 (CH_3-4‴″), 18.76 (CH_3-3‴″). Anal. calcd. for $C_{29}H_{28}N_4SO_2$ (496.19): C, 70.14; H, 5.68; N, 11.28. Found: C, 70.10; H, 5.65; N, 11.22. EI-MS (*m/z*): 496 $(C_{29}H_{28}N_4SO_2)^{\cdot+}$ $(M)^+$, 353 $(C_{19}H_{19}N_3SO_2)^+$, 258 $(C_{13}H_{12}N_3SO)^{\cdot+}$, 239 $(C_{16}H_{17}NO)^+$, 186 $(C_{12}H_{12}NO)^+$, 184 $(C_{12}H_{12}N_2)^{\cdot+}$, 143 $(C_{10}H_9N)^+$, 130 $(C_9H_8N)^+$, 120 $(C_8H_{10}N)^+$, 91 $(C_6H_5N)^+$, 78 $(C_5H_4N)^+$.

N-(3,5-Dimethylphenyl)-4-[({5-[3-(1*H*-indol-3-yl)propyl]-1,3,4-oxadiazol-2-yl}sulfanyl)methyl]benzamide (8k)

Light brown-colored sticky liquid; yield: 77%; mol. formula: $C_{29}H_{28}N_4SO_2$; mol. weight: 496 g/mol; IR (KBr, υ, cm^{-1}): 3282 (N-H str.), 2945 (C-H aromatic str.), 1664 (C═O str.), 1599 (C═C aromatic str.), 1535, 1473, 1456 (str. for oxadiazole), 1155 (C-O-C str.), 1116 (C═N str.), 689 (C-S str.); ^{1}H NMR (600 MHz, DMSO-d_6, δ, ppm): 10.83 (s, 1H, NH-1), 10.08 (s, 1H, CONH), 7.91 (br.d, *J* = 8.1 Hz, 2H, H-2‴′ & H-6‴′), 7.57 (br.d, *J* = 8.1 Hz, 2H, H-3‴ & H-5‴), 7.51 (br.d, *J* = 7.7 Hz, 1H, H-7), 7.41 (br.s, 2H, H-2‴″ & H-6‴″), 7.35 (br.d, *J* = 8.1 Hz, 1H, H-4), 7.14 (s, 1H, H-2), 7.07 (br.t, *J* = 7.3 Hz, 1H, H-6), 6.97 (br.t, *J* = 7.4 Hz, 1H, H-5), 6.74 (br.s, 1H, H-4‴″), 4.54 (s, 2H, CH_2-7‴), 2.88 (t, *J* = 7.4 Hz, 2H, CH_2-1′), 2.77 (t, *J* = 7.2 Hz, 2H, CH_2-3′), 2.26 (s, 6H, CH_3-3‴″ & CH_3-5‴″), 2.06 (quint., *J* = 7.3 Hz, 2H, CH_2-2′). ^{13}C NMR (150 MHz, DMSO-d_6, δ, ppm): 168.09 (C-5″), 164.95 (C-8‴), 162.25(C-2″), 140.21 (C-4‴), 138.91 (C-1‴″), 137.46 (C-3‴″ & C-5‴″),

136.30 (C-8), 134.35 (C-1‴), 128.88 (C-3‴ & C-5‴), 127.81 (C-2‴ & C-6‴), 127.01 (C-9), 125.15 (C-4‴), 122.49 (C-2), 120.86 (C-6), 118.16 (C-7), 118.16 (C-5), 118.09 (C-2‴ & C-6‴), 113.22 (C-3), 111.35 (C-4), 35.34 (C-7‴), 26.47 (C-2′), 24.25 (C-1′), 23.81 (C-3′), 21.08 (CH_3-2‴ & CH_3-6‴). Anal. calcd. for $C_{29}H_{28}N_4SO_2$ (496.19): C, 70.14; H, 5.68; N, 11.28. Found: C, 70.10; H, 5.65; N, 11.22. EI-MS (*m/z*): 496 $(C_{29}H_{28}N_4SO_2)^{\cdot+}$ $(M)^+$, 353 $(C_{19}H_{19}N_3SO_2)^+$, 258 $(C_{13}H_{12}N_3SO)^{\cdot+}$, 239 $(C_{16}H_{17}NO)^+$, 186 $(C_{12}H_{12}NO)^+$, 184 $(C_{12}H_{12}N_2)^{\cdot+}$, 143 $(C_{10}H_9N)^+$, 130 $(C_9H_8N)^+$, 120 $(C_8H_{10}N)^+$, 91 $(C_6H_5N)^+$, 78 $(C_5H_4N)^+$.

4.2 | Alkaline phosphatase assay

Activity of calf intestinal alkaline phosphatase (CIALP) was measured by spectrophotometric assay as previously described.[28,29] The reaction mixture consisted of 50 mM Tris-HCl buffer (5 mM $MgCl_2$, 0.1 mM $ZnCl_2$ pH 9.5), the compound (0.1 mM with final DMSO 1% (v/v) and mixture was pre-incubated for 10 min by adding 5 µL of CIALP (0.025 U/mL). Then, 10 µL of substrate (0.5 mM *p*-NPP (*para*-nitrophenylphosphate disodium salt) was added to initiate the reaction and the assay mixture was incubated again for 30 min at 37°C. The change in absorbance of released *p*-nitrophenolate was monitored at 405 nm, using a 96-well microplate reader ($OPTI_{MAX}$, Tunable USA). All the experiments were repeated three times in a triplicate manner. KH_2PO_4 was used as the reference inhibitor of CIALP.

The alkaline phosphatase activities were calculated according to the following formula:

$$\text{Alkaline phosphatase activity } (\%) = \left(OD_{control} - OD_{sample} \times 100\right)/OD_{control}$$

where $OD_{control}$ and OD_{sample} represent the optical densities in the absence and presence of sample, respectively.

4.3 | Kinetics assay

On the basis of IC_{50} results, the most potent inhibitor **8b** was selected for determining the mechanism of enzyme inhibition. The inhibitor concentrations used were 0.0, 0.0427, and 0.1708 µM. Substrate *p*-NPP concentrations were 10, 5, 2.5, 1.25, and 0.625 mM at 37°C. Pre-incubation time and other conditions were same as described in alkaline phosphatase inhibition assay section. Maximal initial velocities were determined from initial linear portion of absorbances up to 10 min after addition of enzyme at per minute's interval. The inhibition type on the enzyme was assayed by Lineweaver–Burk plot of inverse of velocities (1/*V*) versus inverse of substrate concentration 1/[*S*] in mM^{-1}. The EI dissociation constant K_i was determined by secondary plot of 1/3 versus inhibitor concentration.

4.4 | Hemolytic activity

Bovine blood samples were collected in EDTA that was diluted with saline (0.9% NaCl), and centrifuged at 1000×*g* for 10 min. Erythrocytes were separated and diluted in phosphate buffer saline (PBS) of pH 7.4 and a suspension was made. Test compound solution (20 µL, 10 mg/mL) was mixed with 180 µL of RBCs suspension and incubate for 30 min at room temperature. PBS was used as negative control and Triton 100-X was taken as positive control.[30,31] The % age of hemolysis was taken as by using formula:

$$(\%) \text{ of Hemolysis} = \frac{\text{Absorbance of Sample} - \text{Absorbance of Negative Control}}{\text{Absorbance of Positive Control}} \times 100$$

4.5 | Statistical analysis

All the measurements were carried out in triplicate and statistical analysis was performed by Microsoft Excel 2010. The results are presented as mean ± SEM with 96% CL.

4.6 | Computational methodology: Grid generation and molecular docking

The alkaline phosphatase structure was retrieved from Protein Data Bank (PDB) (www.rcsb.org) with PDBID 1EW2 in protein preparation wizard. The selected crystal structure of protein was preprocessed and minimized using default parameters in Maestro interface. Bond orders were assigned and hydrogen atoms were added to the protein. All four structures were minimized separately to reach the converged root mean square deviation (RMSD) of 0.30 Å with the OPLS_2005 force field. Furthermore, docking experiment was performed against all synthesized ligands and target protein by using Glide docking protocol.[32] The predicted binding energies (docking scores) and conformational positions of ligands within active region of protein were also performed using Glide experiment. Throughout the docking simulations, both partial flexibility and full flexibility around the active site residues are performed by Glide/SP/XP and induced fit docking (IFD) approaches.[32]

ACKNOWLEDGMENT

The current study was supported by Basic Science Research Program through the National Research Foundation of Korea (NRF) funded by the Ministry of Education (2017R1D1A1B03034948).

CONFLICT OF INTEREST

The authors declare no conflict of interest.

ORCID

Muhammad A. Abbasi http://orcid.org/0000-0003-3439-9286

REFERENCES

[1] P. Hardik, D. Nilesh, P. Jagath, P. Bhagirath, *Int. J. Drug Res. Tech.* **2012**, *2*, 225.

[2] S. Agarwal, S. Cammerer, S. Filali, W. Frohner, J. Knoll, M. P. Krahl, *Curr. Org. Chem*. **2005**, *9*, 1601.
[3] J. Hajicek, *Czech. Chem. Commun*. **2004**, *69*, 1681.
[4] M. A. Metwally, S. Shaaban, B. F. Abdel-Wahab, G. A. El-Hiti, *Curr. Org. Chem*. **2009**, *13*, 1475.
[5] M. S. Chande, K. A. Puthamane, P. A. Brave, R. R. Khanwelkar, D. S. Venkatraman, *J. Braz. Chem. Soc*. **2008**, *19*, 42.
[6] M. Amir, S. Shahani, *Indian J. Heterocycl. Chem*. **1998**, *8*, 107.
[7] J. Hazarika, J. C. S. Kataky, *Indian J. Heterocycl. Chem*. **1998**, *7*, 83.
[8] B. S. Holla, C. S. Prasanna, B. Poojary, K. S. Rao, K. Shridhara, U. G. Bhat, *Ind. J. Chem*. **2004**, *43*, 864.
[9] A. Kumar, B. Narasimhan, D. Kumar, *Bioorg. Med. Chem*. **2007**, *15*, 4113.
[10] A. Pau, R. Cerri, G. Boatto, M. Palomba, G. Pintore, W. Filippelli, G. Falcone, F. Palagiano, F. Rossi, *Il Farmaco*. **1997**, *52*, 93.
[11] E. O. De-Oliveira, C. A. Brandt, M. A. B. Da-Silveira, R. A. Glennon, *Tetrahedron Lett*. **2007**, *48*, 6393.
[12] C. Thomas, H. Hubner, P. Gmeiner, *Bioorg. Med. Chem. Lett*. **1999**, *9*, 841.
[13] A. Rana, N. Siddiqui, S. A. Khan, S. E. Haque, M. A. Bhat, *Eur. J. Med. Chem*. **2008**, *43*, 1114.
[14] U. Sharma, D. Pal, R. Prasad, *Ind. J. Clin. Biochem*. **2014**, *29*, 269.
[15] U. Salar, K. M. Khan, J. Iqbal, S. A. Ejaz, A. Hameed, M. al-Rashida, S. Perveen, M. N. Tahir, *Eur. J. Med. Chem*. **2017**, *131*, 29.
[16] M. Díez-Zaera, J. I. Díaz-Hernandez, E. Hernandez-Alvarez, H. Zimmermann, M. Díaz-Hernandez, M. T. Miras-Portugal, *Mol. Biol. Cell* **2011**, *22*, 1014.
[17] A. Sebastian-Serrano, L. de Diego-García, C. Martínez-Frailes, J. Avila, H. Zimmermann, J. L. Millan, M. T. Miras-Portugal, M. Díaz-Hernandez, *Comput. Struct. Biotechnol. J*. **2015**, *13*, 95.
[18] E. R. Vardy, K. A. Kellett, S. L. Cocklin, N. M. Hooper, *Neurodegener. Dis*. **2011**, *9*, 31.
[19] M. Nazir, M. A. Abbasi, Aziz-ur-Rehman, S. Z. Siddiqui, H. Raza, M. Hassan, S. A. A. Shah, M. Shahid, S. Y. Seo, *RSC Adv*. **2018**, *8*, 25920.
[20] M. Nazir, M. A. Abbasi, Aziz-ur-Rehman, S. Z. Siddiqui, K. M. Khan, Kanwal, U. Salar, M. Shahid, M. Ashraf, M. A. Lodhi, F. A. Khan, *Bioorg. Chem*. **2018**, *81*, 253.
[21] G. Hussain, M. A. Abbasi, Aziz-ur-Rehman, S. Z. Siddiqui, M. Ashraf, A. Noreen, M. A. Lodhi, F. A. Khan, M. Shahid, Z. Mushtaq, S. A. A. Shah, *Med. Chem*. **2016**, *6*, 129.
[22] M. Hassan, S. Shahzadi, S. Y. Seo, H. Alashwal, N. Zaki, A. A. Moustafa, *Front. Comput. Neurosci*. **2018**, *12*, 34.
[23] M. Hassan, Q. Abbas, Z. Ashraf, A. A. Moustafa, S.-Y. Seo, *Comput. Biol. Chem*. **2017**, *68*, 131.
[24] M. Hassan, Z. Ashraf, Q. Abbas, H. Raza, S.-Y. Seo, *Interdiscip. Sci*. **2018**, *10*, 68.
[25] M. Hassan, S. Shahzadi, Z. Iqbal, *JSM Biochem. Mol. Biol*. **2017**, *4*, 1024.
[26] P. Llinas, M. Masella, T. Stigbrand, A. Ménez, E. A. Stura, M. H. Le Du, *Protein Sci*. **2006**, *15*, 1691.
[27] J. Iqbal, M. I. El-Gamal, S. A. Ejaz, J. Lecka, J. Sévigny, C.-H. Oh, *J. Enz. Inhib. Med. Chem*. **2018**, *33*, 479.
[28] A. Saeed, G. Saddique, P. A. Channar, F. A. Larik, Q. Abbas, M. Hassan, H. Raza, T. A. Fattah, S.-Y. Seo, *Bioorg. Med. Chem*. **2018**, *26*, 3707.
[29] R. Muhammad, M. Saleem, M. Hanif, M. R. Maqsood, N. H. Rama, K. H. Lee, S.-Y. Seo, *Bull. Korean Chem. Soc*. **2012**, *33*, 3943.
[30] W. A. Powell, C. M. Catranis, C. A. Maynard, *Lett. Appl. Microbiol*. **2000**, *31*, 163.
[31] P. Sharma, J. D. Sharma, *J. Ethnopharmacol*. **2001**, *74*, 239.
[32] R. Farid, T. Day, R. A. Friesner, *Bioorg. Med. Chem*. **2006**, *14*, 3160.

SUPPORTING INFORMATION

Additional supporting information may be found online in the Supporting Information section at the end of the article.

How to cite this article: Abbasi MA, Nazir M, ur-Rehman A, et al. Bi-heterocyclic benzamides as alkaline phosphatase inhibitors: Mechanistic comprehensions through kinetics and computational approaches. *Arch Pharm Chem Life Sci*. 2019;1–14. https://doi.org/10.1002/ardp.201800278